Spiral galaxy lensing

Determining the mass distribution of spiral galaxies with gravitational lensing.

L.V.E. Koopmans[1], A.G. de Bruyn[1,2] & S. Nair[3]

[1]Kapteyn Astronomical Institute, P.O. Box 800, NL-9700 AV Groningen, The Netherlands
[2]NFRA, P.O. Box 2, NL-7990 AA Dwingeloo, The Netherlands
[3]At present: Astronomical Institute "Anton Pannekoek",
Kruislaan 403, NL-1098 SJ Amsterdam, The Netherlands

1 Introduction

Recently Jackson et al. (1997a) made HST V and I-band observations of five gravitational lens (GL) systems, discovered in the CLASS and JVAS surveys. The lensing galaxies appear highly elongated and not very centrally concentrated (Jackson et al. 1997a; Jackson et al. 1997b). It is argued that of the five galaxies, at least four are disk/spiral galaxies and not elliptical/S0 galaxies. Although most statistical treatments suggest that disk/spiral galaxies should not contribute more than 20% to the number of lensing galaxies (Turner, Ostriker & Gott 1984; Hinshaw & Krauss 1987; Maoz & Rix 1993; Kochanek 1996a), observations of the GL systems B0218+357 (Patnaik et al. 1992; Wiklind & Combes 1995; Carilli et al. 1993; Menten & Reid 1996) and B1600+434 (Jackson et al. 1995; Jackson et al. 1997a; Koopmans & de Bruyn 1997; Jaunsen & Hjorth 1997), as well as the observations of the three other GL systems from the CLASS survey, strongly suggest that the fraction of disk/spiral galaxies in these radio surveys should be significantly higher than 20%. One of these three GL systems is B1608+656 (Myers et al. 1995; Snellen et al. 1995; Fassnacht et al. 1996) of which the lens is a massive highly elongated galaxy with a dust lane, or possibly two galaxy which are merging (Jackson et al. 1997b). The other two are B1933+503 (Sykes et al. in preparation; Nair, in preparation), exhibiting a ~ 0.5 axis ratio of both the mass and the surface brightness distributions (Jackson et al. 1997a), and B0712+472 (Jackson et al. 1997c), which appears as an Sa galaxy with axis ratio ~ 0.5, but could still be an S0 galaxy (Jackson et al. 1997b). The concentration indices (Abraham et al. 1994, 1995, 1996; Driver et al. 1995) of these galaxies (except for B0218+357) suggest that B1600+434, B1608+656 and B1933+503 are in the range of normal disk/spiral galaxies and B0712+472 is in the transition region between elliptical/S0 and spiral galaxies (Jackson et al. 1997a).

The observations of these CLASS and JVAS disk/spiral GL systems has recently spurred a number of papers investigating lensing by disk/spiral galaxies (Loeb 1997; Maller, Flores & Primack 1997; Perna, Loeb & Bartelmann 1997; Keeton & Kochanek 1997).

In this paper we first present results on the modeling of the CLASS GL system B1600+434 (Koopmans & de Bruyn 1997). In the second part of this paper some preliminary results of a statistical analysis of the lens properties of a number of spiral galaxy models are presented. We argue that these properties can be used to further constrain the mass distribution of the dark matter halo around spiral galaxies at intermediate redshifts. We will compare the models of B1600+434 with statistical expectations of the fractions of doubles, triplets and quads and conclude that both are consistent with a massive dark matter halo with a small core radius and not extremely flattened ($q_3^{\rm h} \sim f_{\rm h} > 0.5$).

2 Lens models of B1600+434

Observations The GL system B1600+434 was discovered in the CLASS survey (Jackson et al. 1995). An HST I-band observation (Jackson et al. 1997a; Koopmans & de Bruyn 1997) taken in 1996 shows a highly elongated lens galaxy with a prominent dust lane (Figure 1). Moreover, the presence of dust is supported by the large flux ratio difference between the VLA 8.4GHz radio and B to I band optical images, which was also recently suggested by Jaunsen & Hjorth (1997). This is particularly clear in the Nordic Optical Telescope (NOT) B-band image (Figure 1), in which the south-east image (B) has nearly disappeared, likely due to dust obscuration near the galactic plane. A 10 minute R-band exposure taken with the NOT in 1995 and subsequently deconvolved shows again a highly flattened galaxy with an extent of $\sim 2'' \times 7''$ in between the two QSO images (Figure 1). This gives an axis ratio $b/a \approx 0.3$, which is somewhat smaller than the the surface brightness axis ratio of 0.4 derived by Jaunsen and Hjorth (1997) from their (non-deconvolved) NOT images. All observational evidence suggests that B1600+434, together with B0218+357 (Patnaik et al. 1992; Wiklind & Combes 1995; Carilli et al. 1993; Menten & Reid 1996), is one of the strongest cases of being a spiral galaxy lens. The flux ratio in the radio is about 1.25±0.10. The separation between the two images is $1.39 \pm 0.01''$ (Jackson et al. 1995). We estimate from the HST I-band image that image A lies $1.14''$ away from the center of the galaxy and image B $0.25''$. On the basis of the HST I-band image (Figure 1), it appears that the line joining images A and B crosses the center of the galaxy. We assume an error of $\sim 0.05''$ in the distances between the images and the center of the galaxy as a result of the low S/N in the HST I-band image and possibly a small inclination of the galaxy. The redshifts of the lens and source are 0.42 and 1.59, respectively (Fassnacht, private communications). There is a bright companion disk/spiral galaxy (judging from the bar-like structure in the HST and deconvolved NOT images) some $4.5''$ south-east of the lensing galaxy, as well as a smaller highly flattened galaxy $\sim 10''$ west of B1600+434.

In the case of B1600+434, instead of having a near face-on spiral galaxy, as seems to be the case for B0218+357 (Jackson et al. 1997a), we have a near edge-on spiral galaxy. This gives us an excellent opportunity to probe the oblateness of the dark matter halo mass distribution around the lensing galaxy, without having to worry too much about projection effects of the mass distribution, due to an inclination of the lensing galaxy.

Modeling of B1600+434 First we model the lensing galaxy (G1) and the companion galaxy (G2) as a singular isothermal ellipsoid (SIE) and singular isothermal sphere (SIS) mass distribution, respectively. Fixing the position angle and centers of G1 and G2, the only free parameters of this model are the ratio of the velocity dispersions of G2 and G1, $(\sigma_{\rm G2}/\sigma)$, and the axis ratio, f, of the surface mass distribution of galaxy G1.

If we use our estimate of $\sigma_{\rm G2} = 140 - 245$ km/s and $\sigma \approx 200$ km/s (on the basis of the image separation), we find from Figure 2 that $f = 0.4 \pm 0.1$ for the combined stellar+gas+halo mass distribution of G1. For a non-zero core radius we find that f given in Figure 2 always represents a lower limit for the axis ratio of the combined mass distribution of the lensing galaxy G1. Moreover because f represents the axis ratio of the combined stellar+gas+halo mass distribution and $f_{\rm stellar+gas} < 0.3$, we expect the axis ratio of the halo surface mass distribution to be larger than 0.4. So on the basis of this analytical model we conclude that $f_{\rm halo} > 0.4$.

Subsequently we modeled G1 with an exponential disk, deVaucouleurs bulge and non-singular isothermal halo. We went through an extensive range of lens parameters for the mass, axis ratio, scale length of the disk, core radius of the halo of G1 and velocity dispersion of G2. We numerically calculated the velocity dispersion $\sigma_{\rm h}$ and axis ratio $f_{\rm h}$ of the dark matter halo, using a χ^2 minimization method. We have one degree of freedom in the model and therefore take all models with $\chi^2 < 4$ ($\sim 95\%$ of a χ^2 distribution with one degree of freedom) as being a model that fits the observations (image positions and flux ratio) well. Because we use different models with one dataset and not one model with different data sets, we do not expect that 95% of the models give $\chi^2 < 4$. On the other hand a model that gives $\chi^2 < 4$ is a good model with $\sim 95\%$

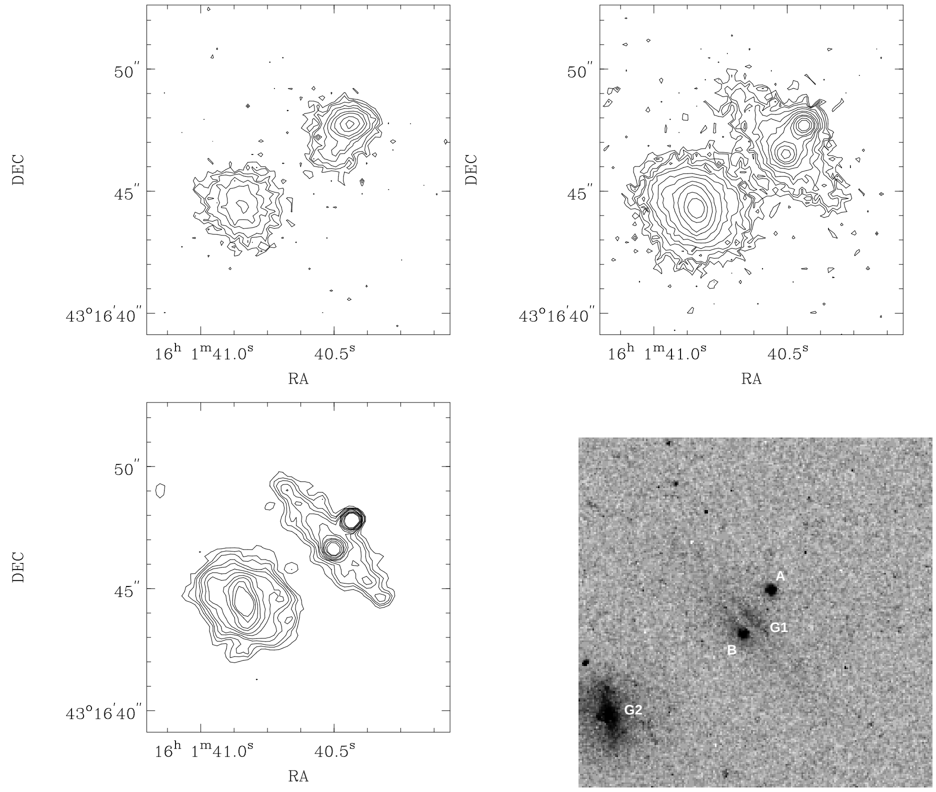

Figure 1: NOT B and R-band images. **Upper left** : B-band image, **upper right** : R band-image, **lower left** : deconvolved R-band image, **lower right** : HST I-band image. North is up, east is left. 1″ corresponds to a physical size of 6.5 kpc at redshift $z_l = 0.415$ and $h_{50} = 1$.

confidence. We also performed these calculations using a Modified Hubble Profile (MHP) for the mass distribution of the halo of G1. The resulting values of $f_{\rm h}$ for all models with $\chi^2 < 4$ are plotted in Figure 2. We find there is a strong dependence of $f_{\rm h}$ on the velocity dispersion of G2. Using the upper limit of $\sigma_{\rm G2} < 245$ km/s, we find that $f_{\rm h} > 0.5$ for all mass models with $\chi^2 < 4$, consistent with our simple analytical model. One of the models is plotted in Figure 2. We conclude on the basis of both analytical and numerical models that the axis ratio of the halo (equal to the oblateness q_3 in case of an edge-on galaxy) has a lower limit $f_{\rm h} > 0.4$. A very flat dark matter halo, as suggested by Olling (1996) ($q_3 = 0.2 - 0.5$), by Pfenniger, Combes & Martinet (1994) and Pfenniger & Combes (1994), is therefore unlikely in the case of G1.

Moreover we find a lower limit on the velocity dispersion of the halo $\sigma_{\rm h} > 140$ km/s, implying that at least half of the mass inside the Einstein radius can be attributed to the dark matter halo. We find a timedelay of $\Delta t_{\rm AB} = (54 \pm 3)/h_{50}$ days for the isothermal halo model and $\Delta t_{\rm AB} = (70 \pm 4)/h_{50}$ days for the MHP halo model. An analytical calculation shows that $\Delta t_{\rm AB}$ is independent of $\sigma_{\rm G2}$ and gives $\Delta t_{\rm AB} = (57 \pm 7)/h_{50}$ days for the isothermal halo model, consistent with the numerical determination. Recent WSRT observations (Koopmans & de Bruyn 1997) show that the lensed QSR of B1600+434 varies $\sim 10\%$ within 3 months and VLA observations show a variation of a factor ~ 2 within a year. Although B1600+434 is a two image system, further constraining the mass model can make B1600+434 a 'golden' lens from which $\rm H_0$ can be determined.

Model	M_d (10^{10} M$_\odot$)	M_b (10^{10} M$_\odot$)	r_c (kpc)	q_3^h
A	10.0	2.50	0.5	1.0
B	10.0	1.00	0.5	1.0
C	10.0	2.50	0.5	0.5
D	10.0	1.00	0.5	0.5
E	25.0	6.25	35.0	1.0
F	25.0	2.50	35.0	1.0

Table 1: The non-fixed mass model parameters. The other fixed parameters are summarized in the text.

3 Statistical analysis of spiral galaxy lensing

In this section we will present some preliminary results of a statistical analysis of a number of spiral galaxy models and compare these results with the results we obtained on B1600+434.

The mass distribution of a spiral galaxy can be constructed out of three distinct mass components: an exponential disk, a deVaucouleurs bulge and a non-singular isothermal dark matter halo. We construct the surface mass distributions for six mass models with nine different inclinations. The asymptotic rotation speed in the galactic plane is chosen to be 250 km/s for all six models, consistent with the rotation speed at $1''$ radius of four of the five galaxies observed by Jackson et al. (1997a). The oblateness of the disk and bulge are $q_3^{\rm disk} = 0.1$ and $q_3^{\rm bulge} = 0.6$, respectively. The scale length of the disk is $h = 7$ kpc and the effective radius of the bulge is $r_{\rm e} = 3.5$ kpc. We assume that $\rm H_0 = 65$ km/s/Mpc, $\Omega = 1$ and $\Lambda = 0$. For all models we assume that the lens redshift $z_{\rm d} = 0.5$ and source redshift $z_{\rm s} = 1.5$. Because we are in the first place interested in the mass distribution of the dark matter halo, we vary the core radius $r_{\rm c}$ and oblateness $q_3^{\rm h}$ of the halo, as well as the disk and bulge masses ($M_{\rm d}$ and $M_{\rm b}$). The values of these parameters are listed in Table 1. The rotation curves of the mass models are shown in Figure 3. Models E and F are maximum disk models, which means that the stellar+gas mass distribution dominates the rotation curve in the inner parts of the galaxy, but also the lensing properties of these galaxies. For models A to D, both the stellar+gas and the halo mass distribution contribute to the lensing properties. We hope on the basis of these GL configurations and models of individual GL systems, to distinguish between the possible mass models of the dark matter halo.

3.1 Results

For all six models and nine inclinations we calculated the lensing cross sections of doubles, quads and triplets, as function of the total magnification (the sum of the magnifications of the individual lens images) and lens image properties (i.e. image separations, flux ratios, etc.). We performed our calculations, using the method described in Blandford and Kochanek (1987). We corrected for the magnification bias (e.g. Turner, Ostriker and Gott, 1984) of the specific set of lens and source redshifts, using respectively the CLASS and JVAS limiting flux densities of 25 and 200 mJy (e.g. Browne et al. 1997). For both surveys the magnification bias for this particular GL configuration with $z_{\rm d} = 0.5$ and $z_{\rm s} = 1.5$ is nearly proportional to the total magnification (Bias $\propto \mu_t^{0.8-0.9}$) and does not change significantly for $z_{\rm s} < 4.0$ (CLASS) or $z_{\rm s} < 3.0$ (JVAS). The magnification bias is calculated using the flat-spectrum RLF of Dunlop & Peacock (1990), following the method described by King & Browne (1996). All our results were corrected using the magnification bias as weight function, which is the reason why all cross sections, $\sigma(\text{property}, \mu_{\rm t})$, were calculated as function of lens image properties and total magnification. For all mass models we have determined the probability distributions of a number of lens image properties, although in this paper we will only present the results on the inferred fractions of doubles, quads and triplets. We will use these in the comparison with the lens models of B1600+434 (Koopmans & de Bruyn 1997).

Ratios of doubles, quads and triplets The fractions of the different image multiplicities (doubles, quads or triplets), normalized by the number of doubles and corrected for the magnification bias is shown in Figure 4. We subsequently averaged over inclination assuming a random orientation of the lens, giving a $\sin(i)$ probability density distribution for the inclinations. We weighted by the cross sections as function of inclination and corrected for the magnification bias in the way described above. Using the cross sections we also calculated the expected average lens inclination, corrected for the magnification bias.

In Figure 4 and in the inclination averaged fractions there are significant differences between the six mass models. Below we have listed the most important results

- Models (A and B) with spherical halo and small core radius are dominated by doubles up to inclinations near $90°$. The inclination averaged fraction of doubles is between 70-80%, the fraction of quads $\sim 20\%$ and the fraction of triplets $\sim 5\%$.
- Models (C and D) with oblate halo and small core radius are dominated by quads at inclinations larger than $\sim 60°$. For model D (moderate bulge mass) triplets will dominate for inclinations $\sim 90°$. The inclination averaged fraction of doubles is about $35 - 50\%$, of quads $\sim 40\%$ and of triplets about $10 - 20\%$.
- Model (E and F) with large core radius will also be dominated by quads and triplets for inclinations larger than $60°$. Averaged over inclination model F will be dominated by triplets ($\sim 70\%$). Quads ($\sim 20\%$) and doubles ($\sim 10\%$) are only a small fraction for model F. For model E the fractions are $\sim 35\%$, $\sim 25\%$ and $\sim 40\%$ for quads, triplets and doubles, respectively.
- The average lens inclination expected for models A and B is $\sim 60°$, for models C, D and E between $65 - 70°$ and for model F about $80°$.

Combined with the probability distribution of lens image properties we believe that the expected fraction of doubles, triplets and quads and the average lens inclination for samples of disk/spiral GL systems, can be used as a tool to determine the likelihood of a particular lens model and to constrain the mass distribution of the dark matter halo around these galaxies, both for individual and samples of GL systems. If the inclination of the lens galaxy is known, the number of degrees of freedom becomes smaller, making it possible to set even tighter constraints on the mass distribution of the dark matter halo. In the next section, we will compare these statistical results with the models of B1600+434.

Comparison of B1600+434 with statistics We can ask the question, what the probability is that a given lens model (seen edge-on) produces a double configuration. If we look at Figure 4 for inclinations near $90°$, we see that the maximum disk models E and F produce $\sim 10\%$ and $\ll 1\%$ doubles, respectively. Model E cannot be excluded entirely, but model F is highly unlikely to produce a double configuration. Model D also produce $\sim 10\%$ doubles. Models A, B and C produce $> 20\%$ doubles. Although we are dealing with only one GL systems seen edge-on, models D to F are not very likely to produce doubles. So on the basis of these statistics it seems that a halo with a small core radius, which is not extremely oblate ($q_3 > 0.5$) is most likely for the double GL system B1600+434. A maximum disk model with moderate bulge mass (Model F) is highly unlikely, because it produces $\ll 1\%$ doubles. This last result is consistent with the fact that we could not fit the image positions and flux ratio with a simple single disk model, having an axis ratio smaller than ~ 0.5, with no halo or massive bulge. A free bulge and disk mass resulted in solutions with bulges that were more massive than the disk. So a moderately oblate halo mass distribution with reasonably small core radius (significantly smaller than the Einstein radius) seems necessary to explain the lensing properties of G1. Although we have compared G1 with the statistics of only six models, we conclude that a very flat ($f < 0.5$) mass distributions (models D to F) are hardly capable of producing significant numbers of doubles, when seen edge-on.

4 Conclusions and future work

If the lens galaxies observed by Jackson et al. (1997a) are disk/spiral type galaxies, this will significantly change our view on the statistical treatments of GL systems. The theoretical prediction that $\sim 80\%$ of lens galaxies are E/S0 galaxies (Turner, Ostriker & Gott 1984; Hinshaw & Krauss 1987; Maoz & Rix 1993; Kochanek 1996a) is contradictory to the high fraction of disk/spiral galaxies in the CLASS/JVAS surveys, although we are still dealing with small number statistics. Not only will a high fraction of disk/spiral galaxies in lens surveys influence statistical treatments, but it will open up the possibility to study the dark matter halo of these galaxies, both statistically and individually. Moreover it can change the constraints set on cosmological parameters, such as the cosmological constant Λ (Kochanek 1996b).

In this short paper we have shown in what way gravitational lensing can be used to determine the mass distribution of the dark matter halo around spiral galaxies. We have also indicated that the expected fractions of doubles, triplets and quads can be used to constrain the mass models of spiral galaxies. Although only the results of six mass models were presented, they show the basic principles which can be used to distinguish between the different mass models. Combining these results with probability distributions of image properties (e.g. flux ratios, image separations, etc) we hope to constrain possible halo mass models even tighter. We have illustrated this using the CLASS lens B1600+434.

In the near future we hope to constrain the mass distribution of the dark matter halo around more disk/spiral galaxies using a combination of modeling individual GL systems and calculating the likelihood of these models on the basis of the probability distributions of their image properties.

Acknowledgments

This research was partially supported by the European Commission, TMR Programme, Research Network Contract ERBFMRXCT96-0034 'CERES'. Furthermore L.V.E. Koopmans and A.G. de Bruyn acknowledge the support from an NWO program subsidy (grant number 781-76-101).

References

Abraham, R.G., et al., 1994, ApJ, 432, 75
Abraham, R.G., et al., 1995, ApJS, 107, 1
Abraham, R.G., et al., 1996, MNRAS, 279, L47
Blandford, R.D., Kochanek, C.S., 1987, ApJ, 321, 658
Browne, I.W.A., et al., 1997, Jodrell Bank Preprint No. CP 5/97
Carilli, C.L., Rupen, M.P., Yanny, B., 1993, ApJ, 412, L59
Driver, S.P., Windhorst, R.A., Griffiths, R.E., 1995, ApJ, 453, 38
Dunlop, J.S., Peacock, J.A., MNRAS, 247, 19
Fassnacht, C.D., et al., 1996, ApJ, 460, L103
Hinshaw, G., Krauss, L.M., 1987, ApJ, 320, 468
Jackson, N., et al., 1995, MNRAS, 274, L25
Jackson, N., et al., 1997a, submitted to ApJ Letters
Jackson, N., et al., 1997b, Jodrell Bank Preprint No. CP 5/97
Jackson, N., et al., 1997c, submitted to MNRAS
Jaunsen, A.O., Hjorth, J., 1997, A&A, 317, 39
Keeton, C.R., Kochanek, C.R., 1997, astro-ph/9705194
King L.J., Browne, I.W.A., 1996, MNRAS, 282, 67
Kochanek, C.S., 1996a, ApJ, 473, 595
Kochanek, C.S., 1996b, ApJ, 466, 638
Koopmans, L.V.E., de Bruyn, A.G., 1997, submitted to MNRAS
Loeb, A., 1997, astro-ph/9701100

Maller, A., Flores, R., Primack, J., 1997, astro-ph/9701110
Maoz, D., Rix, H.-W., 1993, ApJ, 416, 425
Menten, K.M., Reid, M.J., 1996, ApJ, 465, L99
Myers, S.T., et al., 1995, ApJ, 447, L5
Olling, R., 1996, AJ, 112, 481
Patnaik, A.R., et al., 1992, MNRAS, 261, 435
Perna, R., Loeb, A., Bartelmann, M., 1997, astro-ph/9705172
Pfenniger, D., Combes, F., Marinet. L., 1994, A&A, 285, 79
Pfenniger, D., Combes, F., 1994, A&A, 285, 94
Snellen, I.A.G., et al., 1995, ApJ, 447, L9
Turner, E.L., Ostriker, J.P., Gott, J.R., 1984, ApJ, 284, 1
Wiklind, T., Combes, F., 1995, A&A, 299, 382

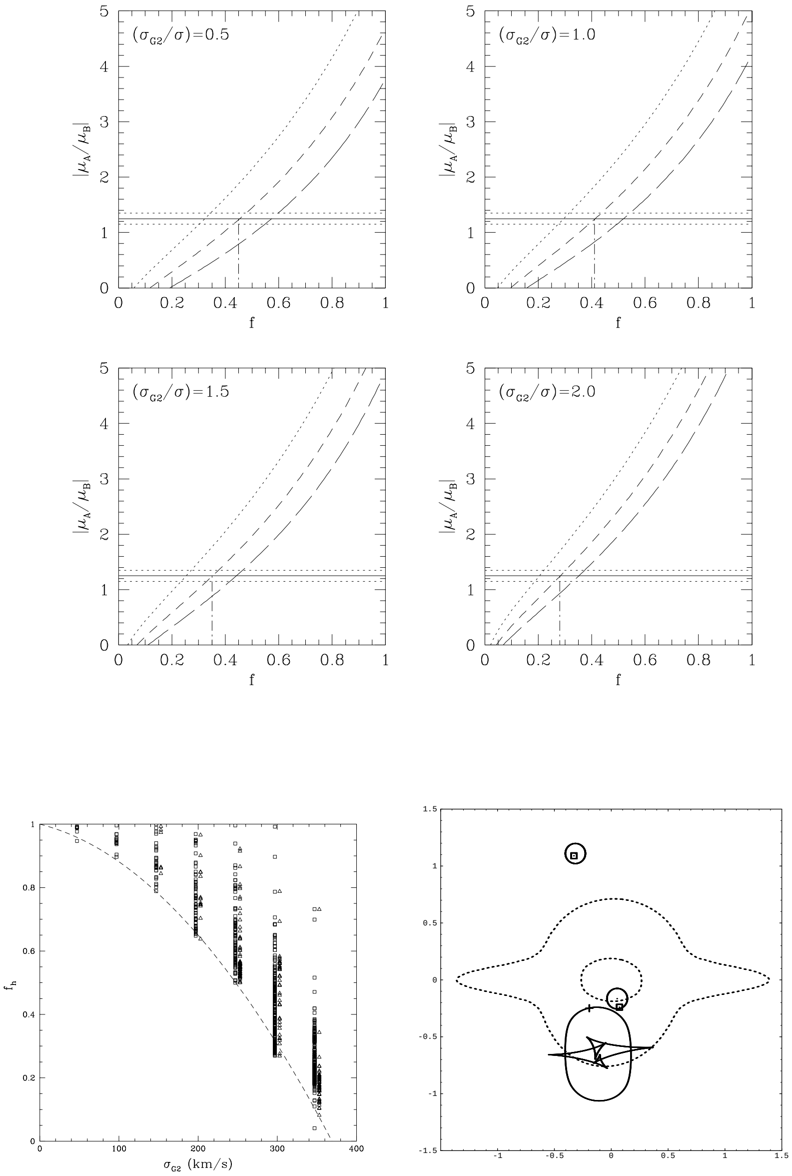

Figure 2: **Top**: The flux ratio $|\mu_{\mathrm{A}}/\mu_{\mathrm{B}}|$ plotted as function of f for $\theta_{\mathrm{B}} = -0.20''$(dot), $-0.25''$(dash), $-0.30''$(long dash) and for $(\sigma_{\mathrm{G2}}/\sigma) = 0.5, 1.0, 1.5, 2.0$, using a simple SIE surface mass model to describe G1 and SIS mass model for galaxy G2. The horizontal solid line gives the flux ratio of 1.25, the dotted lines border the region 1.15-1.35. **Bottom Left**: The axis ratio f_{h} plotted against σ_{G2} for the NIE (square) and MHP halo models (triangle) with $\chi^2_{\mathrm{min}} < 4$. The velocity dispersion σ_{G2} has been shifted by -3 km/s and +3 km/s for respectively the NIE and MHP halo models. The dashed line is the best fit second order polynomial going through the lowest values of f_{h} for each σ_{G2}. **Bottom Right**: The critical lines (dashed) and caustics (solid) for a distinct model of B1600+434 with an non-singular isothermal halo. The circles give the model positions of the lensed images, the area of the circle is proportional to the magnification ($r_{\mathrm{circ}} = 0.05'' \cdot \sqrt{\mu}$). The squares give the positions of the lens images. The cross indicates the calculated position of the source in the source plane. The large shift in the position of the caustics is the result of the presence of G2. We see a model with $r_{\mathrm{c}} = 0.80$ kpc, $f_{\mathrm{h}} = 0.95$, $\sigma_{\mathrm{h}} = 200$ km/s, $h_{\mathrm{disk}} = 4$ kpc, $f_{\mathrm{disk}} = 0.1$, $\mathrm{M}_{\mathrm{disk}} = 5.0 \times 10^{10} \mathrm{M}_{\odot}$ and $\sigma_{\mathrm{G2}} = 200$ km/s. The scale is in arcsecond.

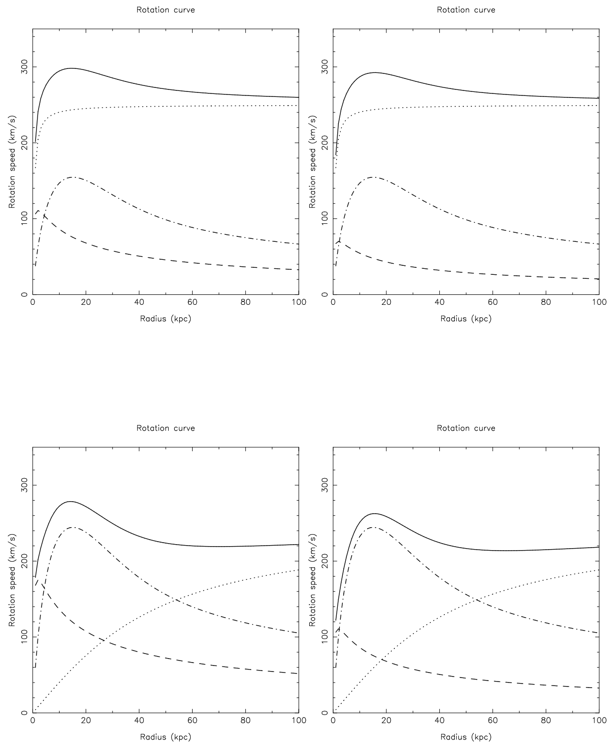

Figure 3: From upper left to lower right : Rotation curves of models A, B, E and F, respectively. The solid curves show the rotation curve of the combined disk, bulge and halo mass distribution. The dotted, dot-dashed and dashed curves give the halo, disk and bulge rotation curves, respectively. The difference between models A and C and between models B and D are insignificant and models C and D are therefore not shown.

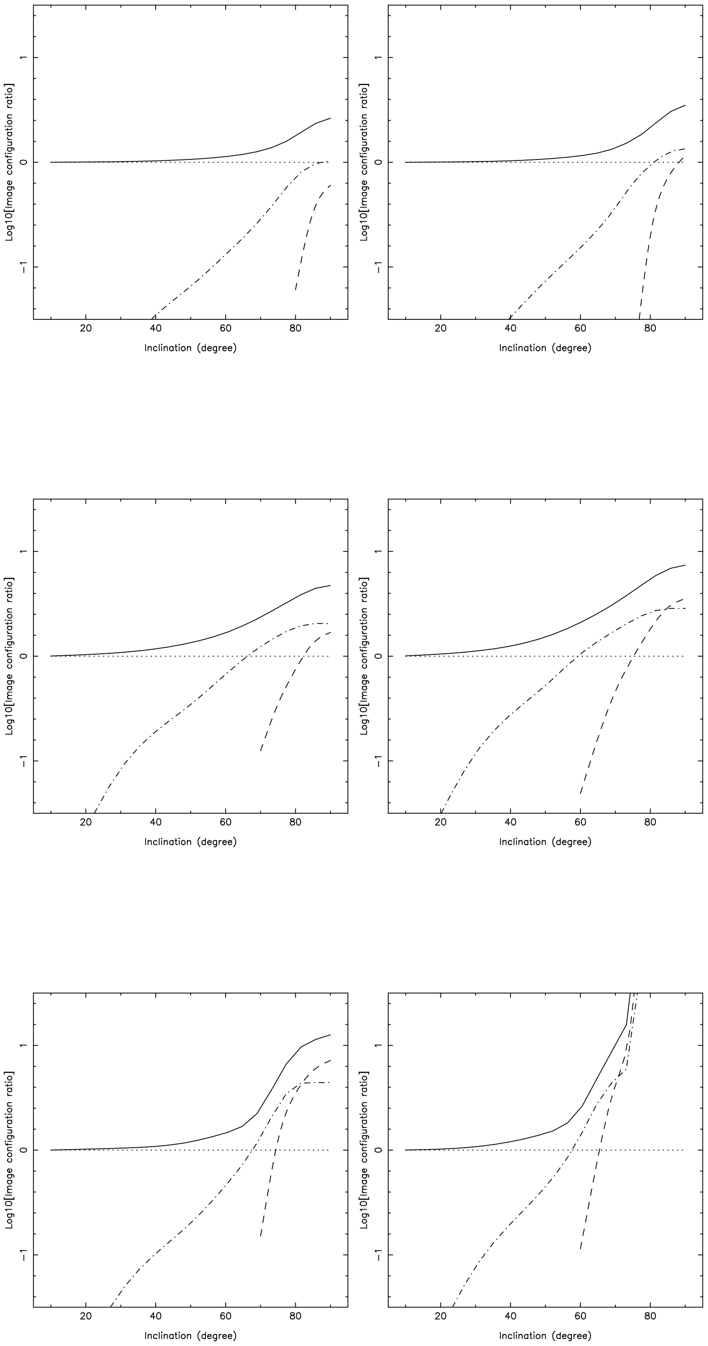

Figure 4: From upper left to lower right : The expected number of GL systems (corrected for the magnification bias) for the different image configurations (doubles, triplets and quads) for mass models A to F, respectively. The normalization is chosen such that the number of doubles is 1.0. The total number of GL systems is denoted by the solid line. The dotted, dashed and dot-dashed lines denote the number of double, triplet and quad GL systems, respectively.